

RADIATION SCIENCE AND TECHNOLOGY | ROTARY WING AIRCRAFT | SANITARY - ENVIRONMENTAL ENGINEERING | STRUCTURAL SEISMIC AND GEOTECHNICAL ENGINEERING | TECHNOLOGY AND DESIGN FOR ENVIRONMENTAL QUALITY IN BUILDINGS AND URBAN CONTEXT | TERRITORIAL DESIGN AND GOVERNEMENT | URBAN AND ARCHITECTURAL DESIGN | VIRTUAL PROTOTYPES AND REAL PRODUCTS | WATER ENGINEERING | AEROSPACE ENGINEERING | ARCHITECTURAL COMPOSITION | ARCHITECTURE, URBAN DESIGN, CONSERVATION OF HOUSING AND LANDSCAPE | **BIOENGINEERING** | BUILDING ENGINEERING | DESIGN AND TECHNOLOGIES FOR CULTURAL HERITAGES | ELECTRICAL ENGINEERING | ENERGY | GEOMATICS AND INFRASTRUCTURES | INDUSTRIAL CHEMISTRY AND CHEMICAL ENGINEERING | INDUSTRIAL DESIGN AND MULTIMEDIA COMMUNICATION | INFORMATION TECHNOLOGY | INTERIOR DESIGN | MANAGEMENT, ECONOMICS AND INDUSTRIAL ENGINEERING | MANUFACTURING AND PRODUCTION SYSTEMS | MATERIALS ENGINEERING | MATHEMATICAL MODELS AND METHODS IN ENGINEERING | MECHANICAL SYSTEMS ENGINEERING | PHYSICS | PRESERVATION OF ARCHITECTURAL HERITAGE | PROGRAMMING, MAINTENANCE, REHABILITATION OF THE BUILDING AND URBAN SYSTEMS



DOCTORAL PROGRAM IN BIOENGINEERING

Chair:
**Prof. Maria Gabriella
Signorini**

The Doctoral Programme in Bioengineering trains graduate students through a strong interdisciplinary education on engineering, mathematics, medical and biological knowledge to develop high level engineering problem-solving abilities in life sciences inside a research group or in private or public industrial context. Students are involved in research works in fields currently ongoing at the Bioengineering Department of Politecnico di Milano which organizes the PhD track.

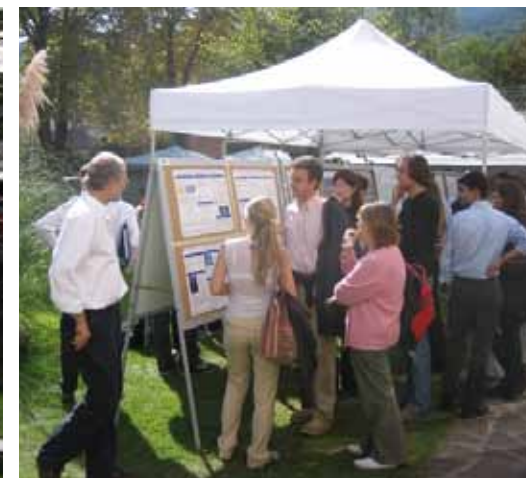
PhD students in Bioengineering are about 15 per year, around 50 in the three year course.

Research themes include modelling and analysis of physiological data, signals and systems; biomedical imaging processing and technologies; technologies and instrumentation for movement analysis, rehabilitation, ergonomics and sports; therapeutic devices and life support systems in cardiology, cardio/surgery and pneumology; design and assessment of prostheses; computer aided surgery and surgery optimization through modelling; cardiovascular fluid dynamics; molecular, cellular and tissue engineering for biomaterials and prostheses; neuro-engineering and nanobiosystems; genomic and proteomic data analysis; bioinformatics. Stage periods in distinguished research institutes in Italy and abroad are an essential feature of the student training.

The educational offer includes ad hoc advanced courses specifically projected for the Ph.D. Among them, the school of the National Bioengineering Group is held every year since 1981 for one week in Bressanone(BZ). The content of the School is focused on themes of the bioengineering research and knowledge and it is organised with the support of national and international qualified teachers in the specific field coming both from academic and industrial research. The school is also a unique opportunity to put together students from different Doctoral Programs coming from the entire country. This allows exchanging ideas and experiences also representing a very useful educational event.

Some themes of the recent past editions:

- 2004** Advanced methods of biomedical signal processing
- 2005** Biomaterials: from prosthetic implants to regenerative medicine
- 2006** Neuro-Robotics. Neuroscience e robotics for the development of intelligent machines
- 2007** Computational Genomics & Proteomics
- 2008** Wearable Intelligent Devices for Human Health and Protection
- 2009** Bioengineering for Cognitive Neurosciences



Scientific and research PhD activities receive a strong support by Laboratories located inside and outside the Department in cooperation with other research bodies and university hospitals:

- Laboratory of 2D-3D analysis and modelling of neural and sensory systems and bioelectromagnetism
- Biomaterials Laboratory
- Laboratory of biocompatibility and cell culture – BioCell
- Laboratory of Biological Structure Mechanics – LABS
- Laboratory of Computational Biomechanics
- The “Luigi Divieti” Posture and Movement Analysis Laboratory
- Laboratory of micro and bio fluid dynamics
- Biomedical Signal Processing Laboratory
- Medical Informatics Laboratory
- Biomedical Technologies Laboratories



The PhD in Bioengineering has an **Advisory Board** which has in charge all the student activities

The External **Reference Committee** is a fundamental link toward the industrial research, the clinical applications with an european and international perspective.

ADVISORY BOARD

Prof. Paolo Francescon (Direttore U. O. Fisica Sanitaria, Ospedale S. Bortolo, Dipartimento di Neuroscienze, Vicenza, Italy)

Dott. Emanuele Gatti (Fresenius Medical Care, Bad Homburg, Germany)

Prof. Ferdinando Grandori (Head Istituto Ingegneria Biomedica CNR, Milano, Italy)

Prof. Antonio Malgaroli, Università Vita-Salute San Raffaele, Head of Molecular and Cellular Physiology Lab, Milano, Italy

Dott. Carlo Mambretti (ASSOBIOMEDICA, Milano)

Dr. Ivan Martin (Head of Laboratory, University Hospital Basel, Institute for Surgical Research and Hospital Management, Basel - Switzerland)

SCHOLARSHIP SPONSORS

Broncus Corp, Canada

Fondazione Giovanni e Annamaria Cottino, Torino

Fondazione MEDEA – Bosisio Parini

IRCCS Fondazione Don Carlo Gnocchi, Milano

IRCSS Ospedale Pediatrico Bambino Gesù, Roma

Istituto di Bioimmagini e Fisiologia Molecolare (IBFM) CNR- Segrate

Istituto di Ingegneria Biomedica ISIB e Istituto di Tecnologie Industriali e Automazione ITIA, CNR, Milano

Istituto Ortopedico Galeazzi, Milano

Italian Institute of Technology, IIT Foundation

Marie Curie project EU

Sorin Group Italia S.p.A., Saluggia

Stazione Sperimentale per la Seta, Milano

In 2010 new PhD positions as **Executive PhD's** have been created. They consist of a special PhD path organized in 4 years and dedicated to PhD candidates that already work in a company/society. The Bioengineering PhD opened 3 positions in 2010.

STUDY OF THE NANOMECHANICAL PROPERTIES OF LUNG EPITHELIAL CELLS AND THEIR ALTERATION IN PULMONARY FIBROSIS MEASURED BY ATOMIC FORCE MICROSCOPY

Irene Acerbi

The framework of this thesis has been the scientific collaboration between the Bioengineering Department of the Politecnico di Milano, and the Unitat de Biofísica of the Universitat de Barcelona. This collaboration is still ongoing, and in fact this thesis work is the starting point for future investigations of the mechanical properties of lung cells in diseased conditions by means of atomic force microscopy (AFM) and other nanotechnologies both at the Universitat de Barcelona and at the Politecnico di Milano.

The lung is a unique organ subjected to several complex mechanical perturbations including breathing movements, pulmonary blood pressure and alveolar surface tension. The main function of the lungs, i.e. the respiratory gas exchange, takes place at the respiratory barrier which includes the alveolar epithelial cell layer and the blood-containing microcapillaries underneath this layer. The above mentioned mechanical stresses in the lung are intimately associated with the normal process of breathing, and are ultimately transmitted from the tissue level to the cellular level. Thus, studying the mechanical response of individual lung cells is essential to understand lung mechanics and function both in normal and

diseased conditions, as many pathologies are associated with dramatic alterations in the mechanics of the lung. Understanding the mechanical response of lung cells is particularly relevant in lung fibrosis and lung cancer, since the mechanical integrity of the alveolar-capillary interphase is dramatically compromised in both diseases. However, the mechanical properties of lung cells in general, and alveolar epithelial cells in particular, in normal and in diseased conditions remain poorly understood, mainly due to the lack of suitable techniques. The recent development of nanotechnologies has offered novel technological opportunities to address the challenges involved in the study of the mechanics of lung cells. Provided with adequate modifications, nanotechnologies are able to mimic some of the mechanical stimuli that affect lung cells and to observe how cells respond to such stimuli, by applying deformations in the range of nanometers and forces in the range of nanoNewtons. Among the different nanotechniques, atomic force microscopy (AFM) has emerged as the most versatile, as it allows probing mechanical properties of biological samples in nearly physiological conditions including

single cells, extracellular matrix gels, and tissue strips. The main goal of this thesis was to provide new insights in the mechanical behavior of lung alveolar epithelial cells in response to biomechanical and biochemical signals that mimic different aspects of normal and pathological conditions. In particular, the alterations of the Young's elastic modulus of lung epithelial cells under the effect of either mechanical stimuli (compression/distension) or biochemical signals (insoluble ligands and pro-fibrotic soluble factors) were studied by AFM provided with suitable modifications. The main goal of the thesis was divided into two specific aims that are summarized below. The first specific aim was to investigate the local resistance to deformation applied in opposing directions on living human alveolar epithelial cells. The rationale underlying this first aim is the fact that alveolar epithelial cells are permanently subjected to cyclic distensible and compressive forces *in vivo* during breathing. However this fundamental mechanical aspect of normal lung function has not been investigated in terms of mechanical responses at the cellular level yet. To address this aim, our experimental approach was to measure the cellular elasticity in response

to compression and distension forces applied locally to the cell surface with AFM provided with a specially nanofabricated nanocylindrical tip. The novel methodological aspects that I implemented to address this first aim include: (i) nanofabricating cylindrical tips with the Focused Ion Beam technique (FIB); (ii) coating the surface of these nanocylinder tips with different peptides; (iii) designing a new measurement protocol to apply local deformation with different directions (compression and distension) on soft samples; and (iv) developing the necessary software tools to control the AFM and to perform the data processing. The measurement protocol was validated on a linear elastic polyacrylamide (pAAM) gel, and was subsequently applied to cultured human alveolar epithelial cells from the A549 cell line. The results showed that, unlike pAAM gels, A549 cells were more deformable to local distension, and less deformable to local compression. Furthermore we identified that the actin component of the cytoskeleton played a major role in the observed differential response. In addition we observed that cells exhibited quick stiffening in presence of extracellular peptide mediated deformations. This quick stiffening may be important as it may contribute to epithelial repair mechanisms triggered upon lung injury. In summary, these data imply that cell mechanosensing depends on the direction of the deformation applied, and thereby indicates that force directionality should be taken into consideration when interpreting

mechanotransduction experiments. The second specific aim was to characterize the stiffening of cultured lung epithelial cells in response to the potent pro-fibrotic soluble factor transforming growth factor beta1 (TGF- β 1), which has been directly associated with lung fibrogenesis as well as with malignant transformation in the lung and in other organs. The rationale underlying this second aim is the fact that abnormal tissue hardening and destruction of the normal alveolar architecture are hallmarks of lung fibrosis, and that the cell types responsible for such stiffening have not been clearly identified. Because TGF- β 1 is a potent pro-fibrotic factor, and it induces epithelial-to-mesenchymal transformation (EMT) in culture, and EMT has been observed in an animal model of lung fibrosis, we hypothesized that cells undergoing EMT may contribute to the abnormal stiffening observed during lung fibrosis. In addition, it should be noted that EMT is a process by which epithelial cells lose epithelial characteristics, and gain mesenchymal properties including expression of cytoskeletal proteins that may confer abnormal contractile properties. To address this aim, I measured the elastic modulus of two different lung epithelial cell models (A549 and H441) untreated or treated with TGF- β 1 for 3 days, and checked for expression of EMT markers by immunofluorescence. These two cell lines were selected based on previous studies that revealed that A549 cells may undergo dramatic EMT upon

proper biochemical stimulation, whereas H441 do not. Our results revealed that TGF- β 1 treatment induced an eight- and three-fold increase in the Young's modulus of A549 and H441 cells, respectively. These findings strongly support that TGF- β 1 may compromise the normal mechanical properties of the lung microenvironment by stiffening epithelial cells. In addition, these results reveal a novel function of TGF- β 1, i.e. stiffening of lung epithelial cells, which may contribute to lung fibrogenesis by altering the normal balance of forces in the lung microenvironment and ultimately compromising lung function. In conclusion, this thesis provides novel measurement protocols based on advanced nanobiotechnological tools optimized for lung cell mechanical measurements, and provides new insights in the basic mechanical properties of the lung alveolar epithelial cells in response to mechanical and biochemical signals that mimic different aspects of normal and pathological lung conditions.

NOVEL STRATEGY AND TOOLS FOR TRACHEA TISSUE ENGINEERING

From the bench to the bedside

Maria Adelaide Asnaghi

End-stage organ failure or tissue loss is one of the most devastating and costly problems in medicine: over 8 million surgical procedures are estimated to be performed every year to treat these disorders in the US alone, incurring a tremendous health care cost of more than \$400 billion annually. Over the last 50 years, tissue and organ transplantations, reconstructive and replacement surgery have significantly improved patient outcomes. Unfortunately, these solutions suffer from many limitations, such as worsening donor shortages, lifelong immunosuppressive regimens, unwanted side effects and finite durability. Therefore, increasing interest has turned to the field of tissue engineering (TE), which applies the principles of engineering and life sciences in an effort to reach a fundamental understanding of structure-function relationships in normal and pathological tissues and to develop *in vitro* biological substitutes able to restore, maintain, or improve tissue and organ function. The basic principle is simple: cells collected from a patient or a donor are either introduced with or without modifying their properties into a three-dimensional supporting material and cultured under proper environmental conditions (i.e.,

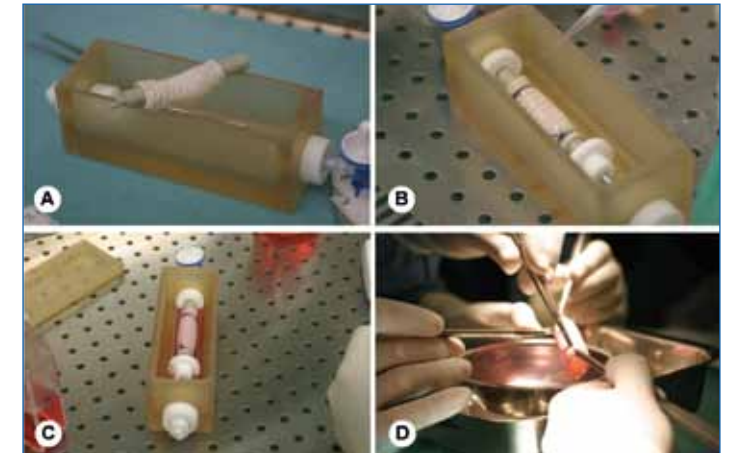
in bioreactors); once the tissue is fully mature or the number of cells adequate, engraftment may be performed. Significant advances have been achieved in the field and examples of successful clinical implementation of tissue-engineered products include skin substitutes, restoration of corneal surfaces, and reconstruction of diseased bladder, providing alternatives to the shortage of suitable grafts for replacement therapies in general and for reconstructive airway surgery in particular. In this field, an unmet need for tracheal replacement exists in the case of extensive defects comprising more than 40-50% of the total length of the organ, since almost every attempt to provide an autologous, allogeneic or synthetic safe and reproducible tracheal graft has been disappointing so far because of stenosis, immunologic complication, and material failure. TE has then emerged as the most promising technique to create a near-normal trachea, and encouraging early experimental results have been reported. In this context, the present study focussed on the development of an integrated approach on all relevant aspects of the TE process toward the definition of an optimal strategy to bring trachea substitutes to the

clinic. In particular, a detergent-enzymatic decellularisation method was applied to a non-immunogenic tracheal tubular matrix of at least 6 cm in length. The protocol was effective, both *in vitro* and *in vivo*, in providing matrices lacking any MHC (major histocompatibility complex) antigens while maintaining structural integrity, therefore a promising substrate for clinical use. To accomplish uniform and highly efficient cell seeding on both the outer and the inner surface of the 3D matrix, co-culturing different cell-types, a novel bioreactor was developed (Fig.1). The bioreactor provides two separate sterile compartments, each with a rotating air-medium interface to promote optimum mass transport between the culture medium and the growing tissue; the rotation also provides the hydrodynamic shear stress necessary to promote cell metabolic activity and proper differentiation. The relative contribution of autologous epithelial cells and mesenchymal stem cells-derived chondrocytes was then evaluated *via* orthotopic implants of bioreactor-recellularised tracheal matrices in pigs, collecting promising results for a successful translation of the approach to the clinic. Ultimate validation of our strategy was provided by the application of this technology

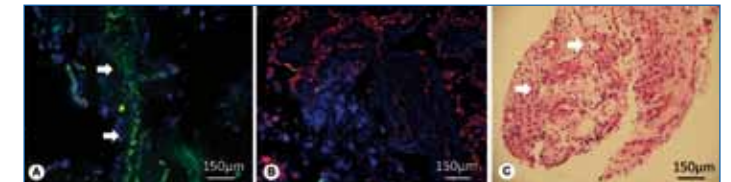
in a 31-year old woman with end-stage bronchomalacia, with permission from all relevant Committees. The recipient had no complications from the operation and was discharged from hospital on the tenth post operative day. The graft immediately provided the recipient with a functional airway (Fig.2) and improved her quality of life, with no immunosuppressive drugs. Cytological and histological studies confirmed angiogenesis and the persistence of viable cells at two months post-surgery (Fig.3). The graft is still functioning well and there is no sign of rejection at 18 months post-implantation. Our clinical experience showed that autologous cells combined with a decellularised donor matrix in a suitable bioreactor could produce a functional tissue-engineered airway, free from the risk of rejection. Our success is highly encouraging, but also serves to highlight the scientific, clinical and commercial bottlenecks standing in the way of full integration of this regenerative medicine technology into routine clinical care, translating our research-scale production model into a clinically applicable manufacturing design that is safe, reproducible, cost-effective, and compliant with the evolving regulatory framework. In an effort to move forward toward this goal and to allow a more efficient use of our bioreactor-based model system in both scientific research and clinically compliant tissue manufacturing, we are developing an advanced bioreactor for simultaneous rotation and luminal perfusion of long tubular scaffolds, and novel

tools to non-invasively monitor and control pH of the culture medium. Whilst focussing on trachea engineering, the developed approach and tools could be efficiently rolled out

for use in other tissues and whole organs regeneration settings.

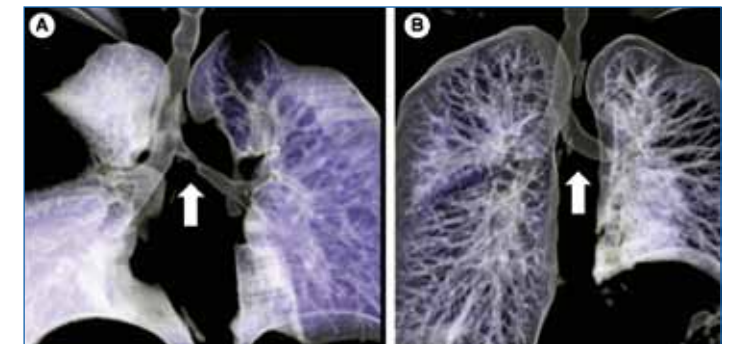


1. Tracheal matrix engineering in the bioreactor and the final graft before surgical implantation



2. Histology of engineered graft biopsies two months after implantation in the patient.

Three-colour immunofluorescence histology: green, cytokeratins 5 and 8; red, collagen II; blue, DAPI (nuclei). A sheet of viable epithelial cells (green) is shown in (A), and many viable chondrocytes (red) are shown in (B). Haematoxylin and eosin image of deep biopsy (C) showing early revascularization



3. Volume-rendering CT before (A) and 1 month after engraftment (B) of tissue-engineered trachea to replace main bronchus.

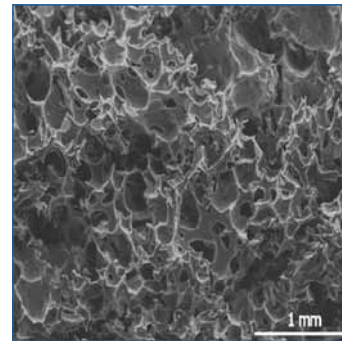
Terminal long segment narrowing is completely reversed after surgery (arrows)

POLYURETHANE FOAMS AND COMPOSITES FOR BONE TISSUE ENGINEERING AND STEM CELLS DIFFERENTIATION

Serena Bertoldi

Numerous efforts are ongoing to develop functional scaffolds for regeneration of tissues and organs, particularly for bone tissue. Natural and biodegradable synthetic polymers have been proposed for the fabrication of scaffolds. Among them, polyurethanes (PU) represent a very important group, thanks to their versatility allowing to achieve a wide range of physical and mechanical properties and making them suitable for use in many areas of tissue engineering, either for reconstruction of soft tissue or for cartilage and bone regeneration. Considering the use of biodegradable materials, a good balance between *in vivo* scaffold degradation and tissue regeneration is not easily achievable. Furthermore, there are concerns about toxic effects imputable to the local concentration of degradation products, that can significantly lower the local pH, inducing a late inflammatory response. Biointegration can be an appealing alternative to biodegradation, and it can be achieved by use of polymeric scaffolds with a very slow degradation rate. In this perspective, the first part of this PhD project was aimed at the synthesis and characterization of biointegrable cross-linked PU foams with slow degradation rate.

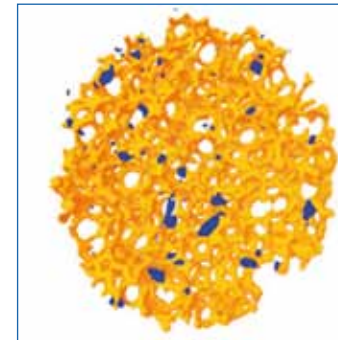
The PU foams were synthesized with a one step bulk polymerization in controlled volume by reacting a polyether-polyol mixture with prepolymer MDI, using Fe-acetyl-acetonate as catalyst, and water as expanding agent. The reaction between water and prepolymer MDI produces carbon dioxide, the porogen agent allowing to obtain the porous structure. On the whole, two families of foams (EC and EF) were developed using two different polyether-polyol formulations, EF-based foams being more hydrophilic than EC-based ones. Figure 1 shows the surface morphology of the obtained foams. Both the foam types have homogeneous morphology and round-shaped pores. For most of the obtained foams, a porosity higher than 50% and an average pore size in the range 200-400 μm were measured, with no differences for the two families. Considering the mechanical characterization, all the PU foams show the typical stress/strain behaviour of elasto-plastic foams, with an initial linear-elastic regime followed by a plateau of roughly constant stress corresponding to the pores collapse. In the dry state all the foams show higher compressive properties than in the wet state, and EF-based foams resulted more flexible than EC-based ones.



1. Representative SEM image of EF-based foams

Higher values of compressive parameters were related to higher density values and lower values of open pores percentage. The repeatability of the synthesis process was assessed synthesizing three foams at the same conditions of temperature and humidity and using the same amount of reaction mixture (50g). All the results obtained by the morphological characterization by micro computed tomography (micro-CT) indicate the good reproducibility of the synthesis process. Therefore, the synthetic procedure proposed in this project turns out to be easy to apply, reproducible, and effective in the production of PU foam adequate for their use as scaffolds for tissue engineering.

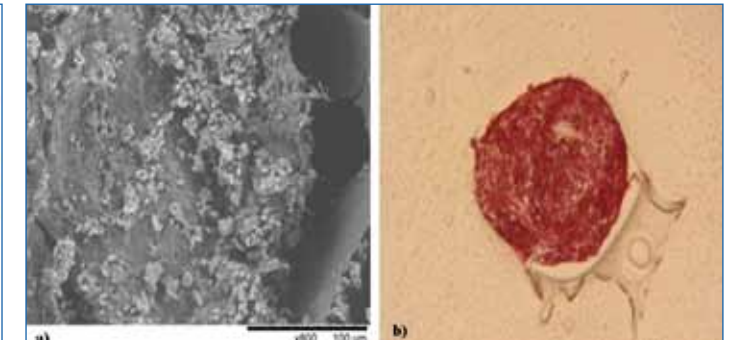
Scaffold for bone tissue engineering should have adequate mechanical properties to support the newly forming tissue. The mechanical properties and the osteoconductivity of the polymeric scaffolds can be improved by the use of calcium phosphate (CaPs), in



2. Representative 3-D reconstruction of EC-based composite with α -TCP. The yellow part represents the PU structure, while the blue one represents the α -TCP particles

particular hydroxyapatite (HA) and tricalcium phosphates (TCP) as filler or coating. In this perspective, the aim of the second part of the project was the production and characterization of composites scaffolds using PU foams as matrices and HA or α -TCP as inorganic fillers and/or coating. The composites were prepared with a co-expansion process, in the presence of α -TCP or HA, adding to the same reagents used for PU foams the proper amount of powder, and/or by coating with CaPs the PU matrices and composites by immersion in a HA or α -TCP suspension. The results obtained by the morphological characterization by SEM and micro-CT indicates a homogeneous distribution of the CaPs particles within the

foam (Figure 2). Adding CaPs during synthesis, in particular HA, allows to increase the mechanical properties of the foams, while the coating with α -TCP can improve materials osteoconduction. Therefore, PU-based composite with HA as fillers and α -TCP coating can



3. Representative SEM image of CMCs cultured onto coated PU foam (a) and histological image of Alizarin red staining of AMCs cultured onto PU foam (b)

be considered the optimal choice for bone tissue engineering application. Besides scaffolds, also cells have key role in the development of engineered constructs. Stem cells hold great promise, and human placenta represents an extremely innovative source of stem cells. Aim of the third part of the work was the evaluation of proliferation and possible differentiation to osteoblastic phenotype of amnion (AMCs) and chorion (CMCs) mesenchymal cells, isolated from human placenta, cultured onto PU foams coated or not with α -TCP. By SEM, a good cells colonization was observed, with cells well adherent within the foam pores, indicating the absence of cells suffering (Figure 3a). The Alizarin Red (Figure 3b) staining assesses the early cells

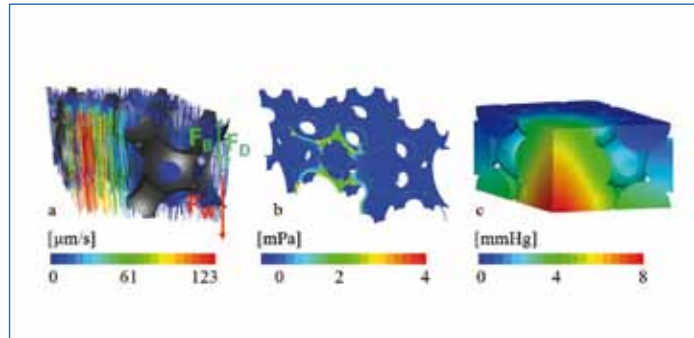
differentiation to the osteoblastic phenotype, thus confirming the basic role of PU foams and composites in supporting AMCs and CMCs differentiation. In conclusion, considering all the obtained results, the described PU-based materials

DESIGN OF A DYNAMIC CULTURE SYSTEM FOR THE IN VITRO MIMICRY OF THE BONE MARROW MICROENVIRONMENT, INTENDED FOR THE EXPANSION OF HAEMATOPOIETIC STEM CELLS

Marco Cantini

Haematopoietic stem cells (HSCs) have been used routinely in clinical practice for more than 3 decades, particularly in the form of bone marrow transplantation, their main indications being haematological malignancies and rescue therapy after high-dose chemotherapy or radiotherapy for non-haematological malignancies. Recent scientific advances have proved that HSCs might be used to treat several other pathologic conditions, including aplastic anemia, thalassemia, sickle cell anemia, and autoimmune diseases.

The difficulty of harvesting HSCs and their scarcity hinder present and expected clinical applications, making the development of systems for their in vitro expansion an appealing prospect for regenerative medicine. The most promising approach for an efficient expansion of undifferentiated HSCs is the mimicry of their physiological microenvironment (the bone marrow): 3D porous substrates should be properly structured for the dynamic co-culture of two different cellular populations, HSCs and bone marrow stromal cells (BMSCs); the latter cells and their 3D organization are expected to reproduce the in vivo physical, cellular and molecular signaling properties of the bone marrow. Considering the cells that have



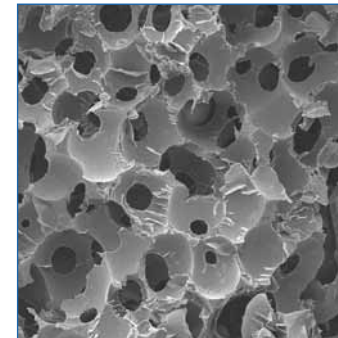
1. (a) Velocity field, (b) wall shear stresses, and (c) oxygen partial pressure of a single periodic unit of channeled 85%-porous scaffold with 300- μm -diameter pores and 1.1-mm-spaced, 450- μm -diameter channels.

to be expanded (non-adherent HSCs), culture conditions and scaffold architecture have to be optimized to allow a proper microenvironment to develop, where non-physiological stimuli leading to HSC differentiation are avoided while guaranteeing nutrient supply to all cells. In the present doctoral project, this issue is addressed through the integration of different methodologies, including computational modeling of the hydrodynamic and mass transport microenvironment, material processing for the manufacture of micro-structured porous substrates for cell culture, and design of a bioreactor system able to host the scaffolds and provide them with controlled culture conditions.

First of all, a model of scaffold characterized by few, simple, effective and fabrication-

related geometric parameters is built, and fluid-dynamic and nutrient transport phenomena within the entire scaffold are modeled using a single representative periodic unit, with minor drawbacks with regard to the reliability of the computed results. The simulations recommend the addition of properly spaced and dimensioned longitudinal micro-channels to an homogeneous porous scaffold as a means to enhance nutrient delivery, maintaining at the same time low levels of drag forces and shear stresses within the porous bulk (τ median ~ 0.08 mPa); moreover, the value of the flow rate to apply to the scaffold is inferred (e.g., 0.02 ml/min for a 6-mm-diameter channeled scaffold, Fig. 1).

Synthetic scaffolds responding to the indications of the numerical studies are produced



2. SEM image of an 85%-porous PCL scaffold

using a polymeric material (polycaprolactone, PCL) and a compression moulding/particulate leaching technique. A fairly reproducible manufacture process is set up and optimized, allowing good control over the scaffold morphology. Using 140 ± 220 - μm -diameter polyethylmethacrylate beads as leachable particles, porous scaffolds are obtained with well interconnected spherical pores and with a porosity that depends on the initial porogen/polymer ratio in a consistent fashion (Fig. 2); longitudinal micro-channels are added by drilling with a numerical control machine. The same optimized technique allows to manufacture bioactive PCL scaffolds containing hydroxyapatite nanoparticles, to promote adhesion and proliferation of the feeder cells. With regard to the dynamic



3. CAD model of a single culture chamber of the bioreactor

culture system, a confined perfusion strategy is chosen, and an easy to handle, versatile, compact, and functional bioreactor is developed and optimized. The idea is the manufacture of a dynamic multiwell, that is a multi-chamber device able to hold several scaffolds at a time, allowing experiments to be carried out in parallel and, in perspective, allowing for a high number of expanded HSCs. The technological solution consists of a modular perfusion chamber with integrated reservoir, hosting the scaffold through an ad hoc designed deformable scaffold holder cartridge (Fig. 3). The device benefits from a closing system similar to the one of commercial T-flasks and from a bayonet coupling between housing and reservoir, that make the assembling of the culture

chamber under laminar flow hood straightforward; the deformable scaffold holder cartridge ensures water-tightness, makes the handling of the scaffold easier, and allows to host scaffolds of different size or shape within the same housing.

Preliminary cell cultures are carried out to prove the efficacy of the manufactured bioreactor at improving initial seeding of feeder cells within 85%-porous PCL scaffolds; an osteoblast-like cell line and primary human skin fibrocytes (model of bone marrow fibroblasts behavior) are used. These cultures represent the first step of a foreseen campaign of cell cultures, that include long term cultures for the repopulation of the scaffolds with feeder cells and for their co-culture with HSCs.

NUMERICAL MODELING OF THE HEALTHY AND PATHOLOGICAL AORTIC ROOT

Application to the analysis of BAV-related alterations

Carlo A. Conti

Bicuspid aortic valve (BAV), the most frequent congenital cardiac malformation, is present in about 1-2% of live births. BAV is thought to result from the intrauterine fusion or non-separation of 2 underdeveloped cusps, the first mechanism being more likely than the second one: usually the right and left coronary leaflet (R/L) or, less frequently, the right coronary and non-coronary leaflet (R/N) are fused. Most of the times, the fusion is characterized by a *raphe*, a region of fibrous thickening at the seam between the two fused leaflets. BAV is widely recognized as a frequent cause of aortic stenosis and/or aortic regurgitation and it is also a risk factor for the development of aortic aneurysms: 50-70% of BAV patients develop ascending aortic aneurysm. The still unidentified genetic defect causing BAV malformation is thought to be responsible for the occurrence of these complications; however, some authors have emphasized the role of altered biomechanics and hemodynamics in the early failure of valve function. The present work aims to gaining insight into BAV function and into its biomechanical implications on the surrounding structures. At this purpose, numerical structural models of the aortic root were developed on the basis of human in vivo

morphometric data, acquired through magnetic resonance imaging (MRI) in collaboration with the Cardiac Surgery Division of the Department of Cardiothoracic and Respiratory Sciences, Second University of Naples, Italy.

Physiological aortic root finite element (FE) model

The geometry of the model is based on MRI data obtained from 10 healthy subjects. The following aortic root main geometric parameters were measured: annulus diameter, commissural positions, width of the Valsalva sinuses, and ascending aorta orientation. As far as tissues mechanical properties are concerned, leaflets tissue was modeled via a transversely isotropic hyperelastic model, while the Valsalva sinuses and ascending aorta tissue were modeled as linear elastic and isotropic. A dynamic FE analysis was performed. The results show that anatomical differences between leaflet-sinus units cause differences in stress and strain patterns. These are notably higher for the leaflets and smaller for the sinuses. For the maximum transvalvular pressure value, maximum principal stresses on the leaflets are equal to 759, 613 and 603 kPa on the non coronary, right and left leaflet,

respectively. Although liable of further improvements, the model seems to reliably reproduce the behaviour of the real aortic root: the model's leaflet stretches, leaflet coaptation lengths and commissure motions, as well as the timings of the aortic leaflet closures and openings, all matched with the experimental findings reported in the literature.

FE modelling of the BAV

The geometry of the model was based on measurements from MR images acquired in 8 normotensive and otherwise healthy subjects with echocardiographically normal function of their BAV. The same tissues mechanical properties implemented for the TAV model was adopted for the BAV one. Numerical results were compared with those obtained from our previous model representing the normal root with a TAV. During systole, the bicuspid valve opened asymmetrically compared to normal, resulting in an elliptical shape of its orifice. During diastole, the conjoint cusp occluded a larger proportion of the valve orifice and leaflets bending was altered, although competence was preserved. The BAV model presented higher stresses with respect to the TAV one, particularly in the central basal region of the conjoint cusp: the

presence of a *raphe* partially reduced stresses in this region, but increased stresses in the other cusp. As regards the proximal part of the ascending aorta, circumferential and longitudinal stresses are increased respectively by 8% and 20% at the intrados and by 17% and 36% at the extrados, when compared to the TAV model. The results show that the aortic valve function is altered also in clinically normally functioning BAVs. Bicuspid geometry per se entails abnormal leaflet stresses: their location suggests that they may play a role in tissue remodeling at the *raphe* region. Morphological anomalies associated to BAV lead to increased stresses not only in the leaflets, but also in all of the surrounding structures. In particular, longitudinal stresses were increased, as compared to the TAV model, in the extrados of the ascending aorta: this stress location is consistent with the region where dilatation associated to BAV is commonly more pronounced. This region is also the most frequent site where aortic dissection occurs. Thus, the mere BAV anatomy, regardless of the possible coexistence of some inherited aortic wall weakness, affects the ascending aorta with altered stress amount and distribution, which may play a role in the onset and development of the quite unique form of aortopathy frequently developing with BAV.

Effects of anisotropy and non-linearity on aortic root and ascending aorta wall modelling

Different thickness and collagen fiber orientations were assigned

to each arterial layer (intima, media, adventitia) of the aortic wall. Layer-specific mechanical properties were defined using an anisotropic non-linear hyperelastic model able to represent collagen fibres dispersion. The coefficients of the strain energy function were obtained from experimental data reported in literature. The mechanical response of the leaflet tissue was modelled with the same strategy previously adopted. The comparison between circumferential and longitudinal stresses in the three layers underlined the anisotropic behaviour of the aortic wall, due to the different orientation of dispersed collagen fibers. An overstressed intimal layer, compared to media and adventitia, was highlighted both in TAV and BAV. In particular, the intimal layer showed levels of circumferential stresses almost two orders of magnitude higher than the middle and the adventitial layer and one order of magnitude higher for the longitudinal stresses.

Comparative finite volume analysis of ascending aorta flow in BAV and TAV

To analyze the fluid dynamics implications of BAV, computational fluid dynamics (CFD) simulations were performed. The system considered for CFD analyses consisted of the aortic root, the ascending aorta, the aortic arch, the supra-aortic vessels and the proximal tract of the descending aorta. In the TAV model, a symmetrical velocity field was computed for the two more proximal considered sections, coherently with the

morphological symmetry of the aortic valve. When the section 2 cm downstream of the STJ was considered, a slight asymmetry was observed: values of velocity magnitude were higher, with a peak value of 1.02 m/s, towards the concavity of the aortic arch. On the contrary, the velocity field computed for the BAV model, was symmetrical at the Valsalva sinus level, but was highly asymmetrical at both the STJ level and mid-ascending aorta level. In particular, at the mid ascending aorta the flow was skewed towards the convexity of the aorta and a peak value of velocity magnitude equal to 1.39 m/s was observed. The study offers preliminary evidence that even normally functioning BAV may generate altered flow patterns. The comparison between TAV and BAV models shows an asymmetrical and higher velocity in the bicuspid one. The asymmetry is more pronounced at the aortic level, known to be more exposed to the early formation of aneurysms in bicuspid patients. This supports the hypothesis that haemodynamic factors may contribute to ascending aorta pathology in this subset of patients.

METHODOLOGICAL DEVELOPMENTS OF THE APPLICATION OF INDEPENDENT COMPONENT ANALYSIS IN EEG-FMRI

Tiziana Franchin

In the last decade, simultaneous acquisitions of electroencephalographic (EEG) recordings during functional magnetic resonance imaging (fMRI) sessions allowed the possibility to greatly enrich the study of the brain functional specialization and integration. The advantages of this multi-modal approach are mainly related to the opportunity of making use of both temporal and spatial resolutions. Established standards of processing and analysis of this sort of data are not defined yet because of several problems still not solved. Independent component analysis (ICA) is an exploratory data analysis approach successfully applied in biomedical data processing, such as the analysis of EEG signals and functional magnetic resonance images. It consists of searching for a linear transformation that minimizes the statistical dependence between its components. ICA consents to analyze the data without a-priori model and the only condition to be warranted is the statistical independence assumption, which is plausibly accepted in the field of biomedical signal processing. The aim of this work is to contribute to the methodological advancement of using the independent component analysis in the

biomedical signal processing. An optimized ICA algorithm was implemented to suggest an alternative and more performing solution to the difficulties related to the computational complexity and to the accuracy of the blind extraction of independent sources. The presented algorithm was used for: removing ballistocardiogram artefacts from EEG recordings in MR field, by means of the extraction of the signal components more correlated with an artefact template; analyzing fMRI data by means of a spatial ICA method to separate more significant components for the identification of functional areas. In blind extraction of independent sources, different algorithms were introduced to solve the problem of a correct recovering of a set of unobservable independent signals from observed mixtures of sources. A possible classification can be feasible considering the problem of the convergence speed and the condition for the separability of linearly mixed source signals. The convergence in the solution recovering is easily attainable with block implementations, which are not necessarily more costly than adaptive (recursive, on-line, sample-by-sample and neural) algorithms: moreover, they are able to use more

effectively the information contained in the observed signal block. The separability of linearly mixed source signals is related to the quantitative measure of non-Gaussianity of the data which is possible introducing an appropriate contrast function. Contrast function is a functional in the distribution of the separator output quantifying a measurable property of the signals and related to the degree of separation. Kurtosis is a well-established measure of non-Gaussianity. Two types of this cost functions exist in this setting. The first one rests on a direct minimisation/maximisation of the kurtosis, which is meaningful only if the variance of the extracted source signal is bounded. The other type of cost function is based on the normalised kurtosis, the advantage of which is that we do not need to perform the otherwise required pre-whitening and weight normalisation operations. The possibility of sparing this pre-processing step makes the components identification faster and more reliable. The proposed algorithm is an optimization of a deflection-mode block-implemented fixed step size algorithm in which the cost function is a normalized kurtosis which considers the effect of noise directly within it. A set of simulation experiments,

differing from the sample size of the synthetic data and the intensity of additive noise, was conducted in order to investigate the performance of the proposed non-parametric method. The convergence speed in terms of the computational cost and the quality of component extraction using this optimized algorithm were compared with the results obtained by the standard version of RobustICA algorithm and by FastICA algorithm, one of the most popular and used ICA algorithm in the bioengineering field. Results showed that the proposed method is truly blind to the particular distribution of the original sources and does not require the selection of optimal working parameters, or suitable non-linearities to act as contrast functions. The optimized ICA algorithm has been successfully used for a better definition of ballistocardiogram (BCG) artefactual components of EEG recordings during fMRI sessions. Auditory and visual ERPs recorded during fMRI sessions were acquired in 7 healthy subjects and used for assessing the method. The source components related to BCG artefacts were separated using three ICA algorithm (FastICA, RobustICA and the optimized algorithm). They were selected computing the linear correlation between the sources and a template created from the ECG recorded signal and an averaged BCG signal. Such selected components were subtracted by raw signals, taking into account the respective estimated weights. For validating the proposed algorithm, a comparing of

the quality of BCG artefact removal obtained by four removal method was carried on by means of: ERP scalp map reconstruction analysis; BCG artefact attenuation percentage; comparison of EEG power spectral density. Despite of the limited available number of subjects, which is a weak point in the validation of the proposed method, the temporal and spectral trend analysis confirmed the quality of the "cleaned" EEG recordings, showing a good reproducibility and comparison of P100 and P200 peaks in and out the MR field. An open challenge in application of spatial Independent Component Analysis for fMRI analysis is the correct separation of components which reflect interesting spatiotemporal patterns of stimulus-induced or spontaneous brain activity from other ones which reflect signal artefacts or noise. An alternative proposal of classification of significant independent components based on the analysis of the spatial features of the signals obtained by fMRI images is proposed. The aim is to implement an easier method for blind identification of cerebral functional areas investigated in single-subject and multiple subject studies. It is characterized by using the above-written optimized algorithm, which consent a good separation of the significant components related to signal information respect to noisy contributions, whose statistical properties are simply identifiable. For this reason, the proposed method was tested on an fMRI group dataset obtained during

a cognitive processes study and on two single cases of different type of epilepsy. Separating components were classified considering the correlation of the independent sources with the spatial template of grey and white matter of the subjects. This first step of classification was followed by the analysis for the kurtosis value of each single component. Components with a high amplitude during a little frequent period and close to zero amplitude for the rest of the time usually own a super-Gaussian random distributions: otherwise, small continuous temporal trends have a quasi-Gaussian distributions. These statistical features are easily distinguished using the kurtosis value. The last step was to mask the significant areas obtained by the over-described sorting components. An automated anatomical labelling of functional activation areas was performed starting by a pre-existing anatomical parcellation atlas: for each spatial IC map identified by the above-written steps, activated areas corresponded to the parcellated ones individuated. Activated areas individuated by spatial IC maps show similar results obtainable with well-established processing method, proving the goodness of the method.

HOME MONITORING OF RESPIRATORY MECHANICS IN PATIENTS WITH CHRONIC OBSTRUCTIVE LUNG DISEASES

Alessandro Gobbi

Asthma and chronic obstructive pulmonary disease (COPD) are the most diffused chronic respiratory disorders affecting millions of children and adults worldwide. Common features of these diseases are the presence of a state of chronic inflammation of the respiratory tract associated to airway obstruction and the periodic onset of acute exacerbations, one of the main causes of patient suffering. In clinical settings, the diagnosis and staging of asthma and COPD still rely on a one time punctual assessment of lung function by spirometry. However, recent findings have suggested that, given the abnormal temporal fluctuations of many respiratory parameters associated with the disease, a proper evaluation of the patient's condition at any point in time would require frequent, at least daily, repetitions of the tests. Up to now, this has been possible mainly with qualitative solutions (diaries, nursery assistance, etc.) while the only quantitative attempt used peak expiratory flow (PEF) meters that, however, provide data with low accuracy and reproducibility. Indeed, even under controlled situations, elderly patients and young children may have difficulty completing spirometry and the supervision of trained technicians is often needed to

obtain results with the desired quality standards. In this work we investigated a different approach for the diagnosis of chronic respiratory diseases, for the association of clinical symptoms to quantitative parameters and for the early detection of acute events. This approach was based on the measurement of the respiratory mechanics (Zrs) by forced oscillation technique (FOT) and on the evaluation of temporal variability of the associated respiratory parameters. Accordingly, we designed a new compact FOT device suitable for the home monitoring of Zrs. This device is able to manage automatically several types of measurement protocols and to guide the patient while making an unsupervised assessment of Zrs. An automatic algorithm is able to compute respiratory parameters in real-time and to identify and discard breaths with artifacts. The results of each test are then encrypted and transmitted over the Internet to a central data server using whichever type of connection available at patient's house (fig. 1). We also designed a database, in which the files sent from each FOT device are memorized and organized. These data can be retrieved from authorized physicians using a web browser from any computer connected to the



1. Home monitoring network architecture

Internet.

The accuracy, stability and repeatability of unsupervised self-measurements of Zrs were confirmed using *in-vitro* validation studies. The device was also tested for a long-term period by monitoring Zrs of one healthy subject and one COPD patient at home for 36 consecutive days. The results showed very limited variations in the healthy subject and a greater variability in the COPD, suggesting that while the respiratory indices are highly stable in the normal, the fluctuations observed in the COPD might reflect a periodic change in airway obstruction. These positive findings and the good results obtained from reliability tests made on the network architecture and on the automatic algorithm for the computation of Zrs allowed to design a more extensive pilot

clinical study, involving a greater number of subjects and recording their Zrs at home for a longer period. Therefore, two age-matched populations of 10 mild asthmatics and 10 controls were included progressively in this study and they were required to make the test daily in the morning and in the evening for at least 6 months. Their measurements were used to build the time series of Zrs. A subgroup of 3 asthmatics and one control were given a portable PEF-meter and they recorded their morning and evening PEF for at least one month. The time series of the PEF were compared to the time series recorded by FOT. The results were unclear, since the correlation between PEF and the mechanical respiratory parameters was significant in some cases but weak or absent in others. These results strengthened our belief that Zrs data might provide a valid alternative to PEF to look at chronic respiratory diseases from several new angles, for a better understanding of the mechanisms of their variability. We compared the global statistical properties (mean, standard deviation and inter-quartile range) of the FOT time series with and without missing data, finding no significant differences between them.

Neither the comparison between the controls and the asthmatics showed significant differences in these global indices, suggesting to analyze at a deeper level the notion of variability, considering different time scales of observation. The variability of Zrs at the smaller time scales, up to several minutes, did not differ significantly between the asthmatic and control group, while significant differences between them were observed starting from the time scale of one day, indicating that two daily tests is the minimum required to separate the populations. Consequently, we calculated the probability of being asthmatic given a relative daily change in Zrs. At time scales greater than one day we were able to correlate the gravity of asthma to the observed variability: the greater the absolute value of variability and its rate of increase with time the more severe the clinical symptoms of the pathology. These results provide a very useful diagnostic tool in situations where the standard spirometric tests are not reliable. Additionally, in asthmatic subjects already under therapy, the home monitoring based on FOT can be conveniently used for a better management of their pathology and for

the evaluation of the effects of the medications over time. From the same time series we also derived the predictor of the likelihood of future exacerbations, given the variability of Zrs measured at a given time scale. Additionally, in a parallel clinical study we found that obesity is associated to an excessive airway responsiveness and variability in otherwise healthy humans. We studied 41 healthy subjects with body mass index (BMI) ranging from 20 to 56. The main results of this study indicated that airway responsiveness was significantly correlated with BMI in nonasthmatic subjects and that this increase was significantly related to lung volume restriction and to an increase of breathing frequency. These findings indicate that obesity is an important clinical factor to take into consideration when analyzing the long-term variability of respiratory parameters in subjects without chronic respiratory disorders. In conclusion, this work showed that a home daily monitoring of respiratory mechanics is feasible and it may contribute to improve the clinical management of patients with chronic obstructive lung diseases.

QUANTIFICATION OF MICROSCOPIC TISSUE DAMAGES IN NEUROLOGICAL DISORDERS

Diffusion Tensor Imaging and Fiber Tracking

Maria Marcella Laganà

Clinical application of diffusion tensor imaging (DTI) and tractography poses challenging problems as to the diversity of brain morphologies to be analyzed in the presence of lesions, diffused damages, or atrophy and also to the deviations of DTI parameters driving tractographic reconstruction. The development and validation of specific protocols were based on a thorough methodological analysis of the single steps and on extended clinical trials on brain and spine structures. Specific aspects dealt with were: the unfavourable SNR of DTI; the limited acquisition times permitted in clinical studies; optimization of registration and averaging procedures; the interference of lesions with tractographic reconstruction; the dependence of reconstructed fibre bundles (tracts) from seeding ROIs; the segmentation of tract volume for the evaluation of micro-structural diffusion by means of individual or atlas based methods. Brain DTI sequence selection, based on SNR and tractographic reconstruction optimization was performed among 26 combinations of scanning parameters evaluated by means of 7 methods for SNR estimate on phantom and human data. Segmentation of bundles was performed by individual and atlas based methods. A procedure for stopping criteria threshold adaptation to microscopic

lesion damages in individual tractographic reconstruction was developed and validated on corpus callosum (CC) tracts in a set of 35 multiple sclerosis (MS) patients. Four Atlas types were constructed from 18 healthy volunteers (HV): A1) linear registration (LR) of diffusion weighted images (DWIs) prior to DTI computation; A2) non-linear registration (NLR) of DWIs; A3) LR of subjects' DTIs; A4) NLR of subjects' DTIs. The simplest atlas, A1, was sufficient for the CC, while A3 was necessary for the reconstruction of peripheral bundles (inferior-fronto-occipital-fasciculus: IFOF; inferior-longitudinal-fasciculus: ILF; Arcuate fasciculus: AcF) (Figure 1). The computationally expensive NLR of HV did not introduce any improvement in atlas reconstruction. Conversely, NLR for the normalization of individual patients to atlas, proved to be necessary both for CC and the other bundles. A clinical study for individual- and atlas-based techniques' performances comparison was performed with the examination of 35 MS patients (14 Relapsing-Remitting, RR, and 21 Secondary-progressive, SP) and 18 HV. The DT-derived metrics (i.e. fractional anisotropy, FA, and mean diffusivity, MD) of the CC WM fibers were computed using the optimized individual-based method for fiber tracking and two atlas-based methods with different

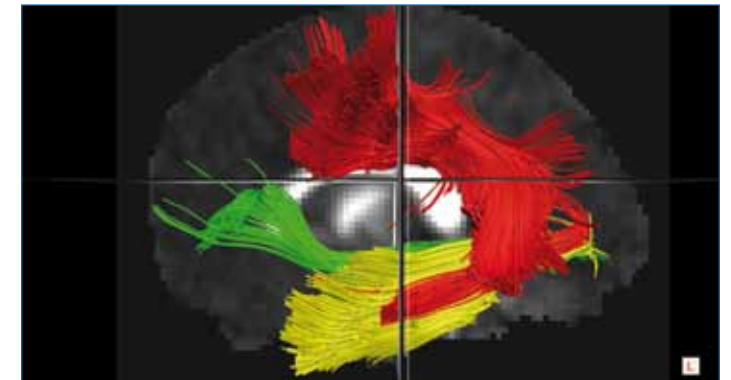
kinds of subjects' registration (LT or NLR) to the atlas A1. All the methods were able to distinguish between MS patients and HV, any statistically significant difference was found between measures derived with individual method and those with atlas A1 and NLR, but using the individual-based tracking method with customized termination criteria, stronger relationships (the highest Spearman's correlation coefficients, Table 1) were found between CC DT-derived metrics and the subjects' clinical condition. Indeed, the Friedman test demonstrated that the magnitude of the observed correlations was greater when using individual-based than when using atlas-based LR ($p=0.003$ and 0.002) and atlas-based NLR ($p=0.04$ for both comparisons) methods. However, the individual-based approach is not without limitations. First of all, MS patients' CC reconstruction was feasible in vast majority (94%) of examined patients (Figure 2 A), but tractography terminated near lesions in 2 out of 35 patients (Figure 2 B). Beside that, while the atlas-based methods are completely automated, the individual-based one can be time-consuming for the operator, due to the manual positioning of ROIs, which is about 15 minutes for an experienced operator. Since the individual-based method is operator-dependent, the intra-rater and inter-rater

measurement dependency was tested with a reproducibility study in a subgroup of 12 MS patients, where the main rater repeated the measurements twice, while a second rater performed the same measurements without being aware of the other rater's results. This analysis demonstrated a very high intra- and inter-rater measurement reproducibility for the average CC DT-derived measures.

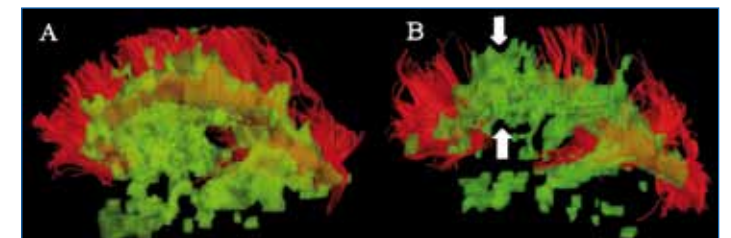
As about the performance of peripheral bundle tractography, it was preliminarily tested on 3 stroke patients with large hemispheric lesions and 3 patients with dementia. In stroke the individual analysis was not appropriate and NLR on A3 best performed. In dementia the individual approach was used to evaluate white matter degeneration accompanying gray matter damage. Preliminary studies were performed for the optimization of DTI in the spine and validated on 11 HV. Nineteen DTI (8 sagittal and 11 axial) sequences were compared for SNR and resolution. A method for DT-derived measures analysis in reconstructed tracts inside, more caudal or more cranial to the lesion level was performed and validated on 3 MS patients with at least one cervical cord lesion: tractography demonstrated to produce indices correlated to pathology or physiology more than the simple and commonly used ROI analysis. In conclusion, this study demonstrates the feasibility of an extension of DTI and tractographic procedures to clinical neurology, through the optimization of DWI sequence and image processing methods, which were applied and validated in specific clinical studies.

	AVERAGE CC FA		
	Individual-based tractography	Atlas-based LT tractography	Atlas-based NLT tractography
Subjects' condition (HV vs RRMS vs SPMS)	-0.83**	-0.65**	-0.72**
	AVERAGE CC MD		
	Individual-based tractography	Atlas-based LT tractography	Atlas-based NLT tractography
Subjects' condition (HV vs RRMS vs SPMS)	0.81**	0.60**	0.69**
** $p < 0.01$			

Tab 1. Spearman's rank correlation coefficients between DT-derived measures computed in CC and the subjects' condition (HV vs. RRMS vs. SPMS)



1. Arcuate fasciculus (red), inferior longitudinal fasciculus (yellow), inferior fronto-occipital fasciculus (green) reconstruction on Atlas 3.



2. A) Successful individual-based tractography reconstruction of the CC from a 43-year old female SPMS patient. The patient has a brain T2 lesion load (LL) of 34.99 ml. T2-visible MS lesions (green) are superimposed to the reconstructed CC. B) Incomplete, individual-based tractography reconstruction of the CC from a 38- old female SPMS patient. The patient has a brain T2 LL of 13.52 ml. T2-visible MS lesions (in green) are superimposed to the partially reconstructed CC and white arrows indicate the premature ending of anterior body fibers.

DEVELOPMENT AND APPLICATION OF COMPUTATIONAL METHODS FOR THE ANALYSIS OF TWO-DIMENSIONAL GEL ELECTROPHORESIS MAPS

Saveria Mazzara

The last decade in life sciences was deeply influenced by the development of the “Omics” technologies (genomics, transcriptomics, proteomics and metabolomics), which aim for a global view on biological systems. Correlating proteomic with genomic information is not an easy task: not only expression levels of proteins vary widely within a cell, but also their correlation with mRNA level is rather poor. In addition, especially in higher organisms, post-translational modifications and differential splicing can significantly hide the information gained at the DNA level. It is thus that proteomics is becoming an emerging area of research in the postgenomic era that deals with the complexity of protein expression via a combination of techniques for resolving, identifying, quantitating, and characterizing proteins. The drive to analyze proteins at a genomic scale has led to the development of a number of parallel approaches. Among them, two-dimensional polyacrylamide gel electrophoresis (2D-PAGE) still plays a central role for analyzing the protein composition of a given cell type and for monitoring changes in gene activity through the quantitative and qualitative analysis of the thousands of proteins that orchestrate various

cellular functions. 2DE provides a proteome mapping of the sample via orthogonal mass/charge analysis. The sample (e.g. tissue, serum) is solubilised, and the proteins are denatured into their polypeptide subunits. This mixture is then separated by isoelectric focusing; on the application of a current, the charged polypeptide subunits migrate in a polyacrylamide gel strip that contains an immobilized pH gradient until they reach the pH at which their overall charge is neutral (isoelectric point or *pI*), hence producing a gel strip containing discrete protein bands along its length. This gel strip is then applied to the edge of a rectangular slab polyacrylamide gel containing sodium dodecyl sulphate, and the focused polypeptides migrate in an electric current into the second gel and are separated on the basis of molecular size. The proteins are represented by spots stained with special dyes. However, converting the large amount of noisy data obtained with 2-DE into reliable and interpretable biological information is still a time consuming process, thus, there is an increasing need of fully automated approaches. Objective of the project has been to develop complementary approaches aiming at an automatic extraction of the

essential information emerging from separation images intended as fingerprints of the correspondent biological conditions able to identify potential discriminant patterns between different clinical/biological conditions. What we would like to propose is a new diagnosis criteria that overcome the diagnostic methods based on single or few marker/s, using a statistical multiparametric analysis. To this aim, image descriptors are derived, on the basis of the extracted quantitative parameters to be used in the successive exploratory analysis. In this way, each gel image, represented as a vector of quantitative features, can be investigated by means of appropriate analytical tools. The development and application of computational methods to the data generated by two-dimensional electrophoresis represents an exciting way to explore the pathophysiological processes at the molecular level; multivariate methods like principal component analysis (PCA), partial least squares (PLS) and local tangent space alignment (LTSA) have been used to analyze several two-dimensional gel electrophoresis datasets. In the present project it is demonstrated how information can be extracted

by multivariate data analysis to efficiently analyze the amount of data generated by 2DE; these techniques are applied on the quantification parameters, obtained through the commercial software, at the aim of exploring the reliability of the features extracted from the experimental subregions of the separation images and providing the bases for a protocol of automatic classification. The processing of the descriptors corresponding to different regions of the separation area can provide the identification of portion of image, and thus subset of spots, that are most responsible in the observing the existence of clusters of samples. In this way it is possible to go back to the ranges of *pI* and MW that are most informative and that most contribute to the analytic representation that shows gels corresponding to different clinical conditions as positions confined in different zones of the new space of observation. In this sense, the developed tool may represent a further support to the identification of potential pathological markers through the selection of critical patterns of image gel. The outlined strategy was tested on three datasets: samples from prostatic cancer tissues, samples of human cerebrospinal fluid (CSF) acquired within a framework of a study of peripheral neuropathy and samples of human CSF acquired in a study on amyotrophic lateral sclerosis. Cancer research is a highly suitable area for the application of such an approach. This is because in many cases it is possible to make a direct comparison of proteins

expressed in control and diseased tissues. The comparison of 2DE separation of such tissues can highlight proteins that are present in greater or lesser quantities and new proteins which may only be expressed in cancerous samples. Such approach appears particularly toward for the characterization of the brain proteome under normal and disease condition; biomarkers of brain disorders are urgently needed to aid diagnosis, monitor disease progression, and, as new medicines are introduced, detect the patients response to treatment. In conclusion, it is worth noting that the samples of the data set are not technical replicates, i.e. gels obtained from fractions of the same biological sample. In this work, biological replicates were processed, i.e. each gel image is representative of a different human subject, so the gels are characterized by low homogeneity; this brings the tackled problem to a much higher level of variability and complexity. Moreover, there exist a difficulty of the reperiability of samples, in particular for control subjects. Notwithstanding these critical aspects, the strategy developed, based on techniques of multivariate analysis applied on the quantification parameters obtained through the commercial software, gave promising and reliable results. The use of 2D gel–electrophoresis coupled to multivariate data analysis seems to be promising as a fast, reliable way of transforming many gels into spot quantities. The method developed can be a useful complement in the routine of a proteomics laboratory,

because it is highly repeatable and does not need any “a priori” information. It may provide an effective visualization tool and lead to the definition of a protocol of automatic classification, that is able to show discriminating patterns within a pool of gels from a clinical/biological study in which quality and reproducibility are challenged by the presence of samples not obtained ad hoc, capturing the fingerprint leaved by the sample on the two dimensional separation image. Moreover, this kind of analysis may provide an useful support in the identification of the most informative areas (spots or groups of spots) that have the major discriminant power between different clinical conditions towards the definition of new potential biomarkers. Finally, nobody expert eye is able from a visual inspection of 2D electrophoretic gels to discriminate physiological from pathological conditions; thus, the information extraction in the processing of 2DE images is an important topic in computational biology and the proposed strategy may provide an interesting and fruitful point of view capturing the essential information from gel images.

DEVELOPMENT OF AN EXPERT SYSTEM BASED ON ARTIFICIAL NEURAL NETWORK FOR BIOMEDICAL EQUIPMENTS' RISK ASSESSMENT

Matteo Ritrovato

In today's health care services biomedical technologies play an exceptionally relevant role: ubiquitous and essential to modern clinical procedures, are one of the main keys for health practices improvement, not only because of the better diagnostic and therapeutic capabilities, but also due to the increased health accessibility, and therefore for the improvement of the *outcome*, as well means by which we have developed research and knowledge in medical sciences. However, there is a downside: the state of functioning and conservation of these devices affects the outcome and safety of procedures; the pace of technological innovation has increased the complexity of use and management, as well as the magnitude of associated costs. Moreover, the complexity and the intrinsic riskiness of each unit are capable to interact in those contexts that require, for the specific clinical procedure, the convergence and integration of different devices, thus increasing the criticalities related to patients and operators safety. The assessment of risk associated with medical devices in general and in particular with biomedical equipments, has thus become an increasingly recognized activity by end-users and managers, both for the implications on patient safety

and for those associated with the management of medical devices. The risk assessment method here developed is based on traditional methods of risk computation: the value of risk associated with a medical equipment or biomedical technology is the product of two factors: the factor Probability (estimated occurrence frequency of potentially damaging event) and the factor Damage (type and extent of damage associated with each event). Thus, the calculated risk value is mapped on a risk matrix and associated to an operational meaning corresponding to an Acceptable, Tolerable and Intolerable risk. To separately compute Probability and Damage factors, we referred to a linear model, previously developed by a working group of the Italian Association of Clinical Engineers and here updated with the contribution of the Clinical Engineering Service at Pediatric Hospital Bambino Gesù and fellow experts, that identifies and quantifies the variables that separately contribute to those factors. The main objective of this work was to overcome the obvious limitations of the initial model, limitations due to its linearity, thus solving the recognized underestimation of the value of

risk associated with many specific combinations of input variables. This goal was approached by implementing, as computational method, two neural networks, one for the calculation of Probability, one for the calculation of the Damage. Therefore, in accordance with the classical method of risk estimation two separate neural networks were implemented, each consisting of one input layer, one hidden layer and one output layer. As transfer function of neurons constituting the input and hidden layers we used a sigmoidal function (whose output is limited to the range $-1 \div +1$), whereas for the output layer, consisting of a single neuron, the function is linear, since the output of each network has to vary in the range $0 \div 4$. The neural network dedicated to the estimation of the probability of occurrences has no. 16 inputs, while the network that computes the value of Damage processes no 6 input variables. The data used for the training phase of the two neural networks are the result of simulations performed on the basis of linear mathematical model from which we started. The data thus obtained were added to those attributed to particular configurations of the input variables that, although

the linear model is not able to indicate as highly risky, has been associated with a high degree of risk on the basis of the opinion of experts. In this way we introduced the non-linearity useful to overcome the limitations of classification of the linear model. The training of the neural network is based on a combination of two algorithms: the first, chronologically, is a genetic algorithm whose objective is to identify an initial configuration of weights of the network sufficiently close to an absolute minimum of error function defined for the network. The second algorithm, given the number of layers and the differentiability of the error function, is a classic backpropagation algorithm. Using a genetic algorithm as a first step in the process of network training, it has become necessary due to the great dependence on initial (random) parameters given as input to the training algorithm based on backpropagation and consequent instability shown by the trained network. At the end of the genetic algorithm, i.e. when the average value of the fitness function given by the entire population of strings converge to the minimum value of the same function given by an element of the population itself (called best individual), it is identified the set of parameters to be passed as initial configuration of the neural network to the next phase of training, phase in which backpropagation algorithm is used. The results indicate that the use of a genetic algorithm has successfully guaranteed, in all

the performed tests, a correct and stable training of the network. Backpropagation algorithm implemented uses the Levenberg-Marquardt algorithm for updating the synapses' weights, and as error function the mean square error. For better generalization, besides limiting the number of neurons forming the network (to avoid the overfitting problem), an early stopping mechanism was used (to avoid the problem of memorization). The simulation of synthetic data, the neural networks, and the training algorithms have been implemented in MatLab 7.0. The expert system was tested on a set of about 180 equipment used at the Pediatric Hospital Bambino Gesù. The average value of risk identified was equal to 3.4, with a variance equal to 2.6. Specifically, we obtained an average value for the damage of 3.2 and a variance of 1.2, while the probability average value was equal to 1.06 and variance 0.12, with only 1 device with risk value >8 (limit of risk "intolerable") and 4 devices with risk value >4 (limit of risk "tolerable"). These 5 devices were subjected to the necessary repairs and improvements so that the recalculated risk returned back within the range $1 \div 4$ (acceptable risk). Moreover, such results were also taken into account in the preparation of the technology replacement and renovation plans. From the monitoring work conducted for 24 months following the initial acquisition of data, with the aim of assessing the ability of

classification of the expert system, there was a minimum (depending on how the risk classification "tolerable" have been considered) specificity equal to 0.97 and a Negative Predictive Value of 1, while nothing can be said about sensitivity, because no adverse events associated with the examined equipments have been occurred. Marginally with respect to such aspects and since during the phase of data acquisition on the set of equipment under investigation there was a clear judgment variability, among operators who have tested the method, while associating values to the variables required by the model, it was investigated the possibility of exploit the potential of fuzzy logic and systems in order to reduce the inherent subjectivity of the expert system. It was therefore implemented a fuzzy system that acts as a layer of data preprocessing. In particular, the data being processed by the fuzzy layer are those relating to subjective assessments of factors not instrumentally measured, required by the neural network that calculates the probability of occurrence, for a total of no. 7 input variables. Therefore it has been defined no. 3 membership functions for each data input, a set of fuzzy rules and operators for the composition of fuzzy set and, finally, the operator of output defuzzification.

REGIONAL ANALYSIS OF LUNG DENSITY FOR PLANNING AND EVALUATION OF ENDOBRONCHIAL INTERVENTIONS IN SEVERE EMPHYSEMA

Caterina Salito

Emphysema is a worldwide leading cause of morbidity and mortality. As defined by the American Thoracic Society, emphysema is “a condition of the lung characterized by permanent, abnormal enlargement of airspaces distal to the terminal bronchiole, accompanied by the destruction of their walls”. Emphysema is characterized on computed tomography (CT) by the presence of areas of abnormally low attenuation. CT, in particular, volumetric acquired high-resolution CT (0.6 to 2 mm collimation) is excellent in detecting the presence and in demonstrating the pattern, distribution, and extent of emphysema. HRCT scans of emphysema patients can be and have been used to identify regions of trapped gas. Definitive therapy for severe emphysema is limited to invasive and expensive surgical measures: lung transplantation and lung volume reduction surgery. Recently a new minimally invasive surgical intervention, airway bypass, has been introduced. This intervention is constituted by the placement of bronchopulmonary conduits, stents, between conducting airways and emphysematous lung parenchyma for expiration. The success of the technique strongly depends on the possibility to identify regions of

trapped gas for interventional target areas. In this Thesis a set of new methodologies and techniques specifically developed in order to identify and quantify regional trapped gas on a lung regional basis is described. The same methods can be usefully used also for surgical planning, namely the choice of the target sites for airway bypass intervention. Here below, a list of more detailed specific aims of this Thesis is reported.

Specific Aim 1 - To identify and quantify regional trapped gas in human lung with severe emphysema via HRCT at disparate lung volumes. Air trapping reflects the retention of excess gas in all or part of the lung and is detected as decreased attenuation on expiratory CT as compared with the corresponding inspiratory images. The methods proposed is addressed to measure the changes in specific gas volume, i.e. the volume of gas per gram of tissue (SV_g , ml/g), as lung volume decreases from a high volume close to total lung capacity (TLC) to a lower volume close to residual volume (RV) by using HRCT. Lobar and overall SV_g were measured by HRCT scanning at total lung capacity (TLC) and at residual volume (RV) in a group of patients with severe emphysema and healthy control subjects. The study

allowed to determine regional distribution of specific gas volume, which can be eventually taken to identify target regions for fenestrations. We found that interlobar heterogeneity in lung emptying was highly variable between patients with severe emphysema. Thus there are patients with large inter- and intralobar regions of gas trapping that act like bullae. Mean SV_g was 3-fold higher than normal. Gas trapping predominates in upper lobes with less decrease in SV /unit decrease in lung volume compared to lower lobes.

Specific Aim 2 - To verify, on an ex-vivo controlled model of airway obstruction, if specific gas volume measured from CT images, can be a reliable estimate of regional gas trapping. In order to utilize high resolution CT scanning and ^3He MRI and apply them to the regional quantification of trapped gas in an unambiguous way to test the techniques, we developed a model of airway obstruction and trapped gas in explanted porcine lungs, which lack collateral ventilation between lung lobules. Dynamic expiratory thin-section CT and ^3He MRI were performed during passive deflation from total lung capacity after obstructions were created with inverted, one-way

endobronchial exit valves in segmental or lobar bronchi, to produce identifiable regions of trapped gas in four porcine lungs removed after sacrifice for unrelated cardiac experiments. Changes in SV_g were assessed from CT data for defined regions of interest (ROI) within and outside of the obstructed segments and for entire lobes. ^3He data were analyzed by the corresponding regional signal reduction during expiration, compared to the total magnetic moment at each time point. The obtained results demonstrate that both CT-determined SV_g and ^3He MRI can identify and quantify the extent of regional trapped gas in explanted porcine lungs.

Specific Aim 3 - To determine the effects of extremely low attenuation values on the calculation of specific gas volume for the assessment of emphysema and gas trapping. Being SV_g defined as the inverse of the lung density (minus a constant which is assumed to be the specific volume of lung tissue), it is highly sensitive to very low attenuation values. Very low attenuation values frequently occur in the case of severe emphysema, where the density of the lungs is much lower than that of water or bone and falls in a range where not all manufacturers have optimized their scanners. In the present Thesis we therefore investigated, for emphysematous and non emphysematous lungs, in-vivo and ex-vivo, the influence of the extremely low attenuation pixel values on lung densitometry, more specifically on specific gas volume calculation (which

is extremely useful for the assessment of emphysema and gas trapping). Different sets of in-vivo and ex-vivo CT lung images were analyzed at two different volume, high and low. In order to evaluate the incidence of very low attenuation pixels on the calculation of the specific volume of gas and reduce the disproportionate weighting of these very low attenuation pixels in specific gas volume assessment, we calculated average values of SV_g by reassigning all pixels below a given Hounsfield value a threshold value. This threshold varied between -1023 and -1000. We found that a significant number of pixels with very low attenuation values are present in the emphysema patient both at TLC and RV. This is not the case in the healthy subject histograms. As expected, SV_g values were significantly higher in patients with emphysema than in the healthy subjects, at both TLC and RV. In emphysema patients, absolute SV_g values were significantly influenced by the threshold applied, on the contrary for healthy subjects, SV_g was not significantly influenced by the threshold. The difference between the ex-vivo and in-vivo SV_g values was remarkably small. Our results show that, in emphysematous but not in healthy lungs, SV_g is significantly affected by very low attenuation values and this effect is emphasized when smaller regions of interest are considered.

Specific Aim 4 - To develop a system for 3D airway tree reconstruction by HRCT images

specifically addressed to the registration of images at different lung volumes in severe emphysema. The work presented in this part of the Thesis is divided in two parts: airway segmentation and quantitative measurements. The first step was to develop a set of new algorithms based on three-dimensional region-growing methods, able to reconstruct the airway tree from the CT datasets. The branch-based region growing algorithm recognizes branch points during the region growing process, and provides as output a binary tree structure. After airway tree segmentation obtained at two different lung volumes, RV and TLC, the software allowed to choose corresponding branches on the two airway trees, particularly those corresponding to all the segmental bronchi which are suitable for airway bypass procedure. For each site a ROI at both lung volumes was then analyzed in terms of HU and SV_g density histograms and mean SV_g and ΔSV_g . The developed algorithm allowed to reconstruct in a successful way the airway trees in both healthy and severe emphysematous lungs, always reaching at least the 3rd/4th bronchial generation. The results obtained in the different ROIs confirmed the general behavior of the lung in terms of HU and SV_g variations.

NEW METHODS FOR THE OPTIMIZATION OF MECHANICAL VENTILATION IN RESPIRATORY DISTRESS SYNDROME (RDS)

Emanuela Zannin

Acute Respiratory Distress Syndrome (ARDS) is a specific form of respiratory failure characterized by diffuse alveolar damage, associated to inflammation and increased permeability of the alveolar-capillary membrane. Infant Respiratory Distress Syndrome (IRDS) is another cause of respiratory failure due to surfactant deficiency and structural immaturity of the lungs.

Although mechanical ventilation is crucial for survival in both adults and infants affected by RDS, if it is not administered adequately it may cause a secondary ventilation induced lung injury (VILI).

Thus the goal of any ventilation strategy should be not only to support but also protect pulmonary function and structure. Any ventilatory strategy addressed to RDS patients should open the lung and maintain alveolar volume, avoiding overdistension and preventing cyclic shear-stress associated with intra-tidal phenomena. However how to achieve this goal remains controversial.

The assessment of lung function has been largely studied for the optimization of ventilatory settings. However all the currently available methods for lung function testing have some problems that limit their

use in the clinical management of ventilated patients. Thus a proper tool able to guide the clinician in tailoring the ventilatory strategy on the individual patient is still missing.

The aim of the present work was to develop new methods able to accurately monitor lung function in ventilated patients and to guide the physician in the optimization of the ventilatory strategy both in adults and infants with respiratory distress.

Forced oscillation technique (FOT) and optoelectronic plethysmography (OEP) have been used and adapted to suit specific clinical applications related to the management of mechanically ventilated patients. FOT is a simple non-invasive technique for the assessment of respiratory mechanics.

It provides a measurement of the respiratory system impedance (Zrs), which is a complex number that can be split into a real part called resistance (Rrs) and an imaginary part, called reactance (Xrs), that describes the compliance and inertance of the system.

At first we evaluated the ability of Xrs measured by FOT at 5 Hz to identify lung volume recruitment/derecruitment. A very strong correlation was found between Xrs and the amount of non-aerated tissue measured by CT scans,

indicating that Xrs is able to quantify changes in lung volume recruitment/derecruitment associated to different interventions affecting lung volume.

Then we tested the ability of Xrs to identify the optimal Positive End-Expiratory Pressure (PEEP). Xrs was able to identify PEEP-induced recruitment/derecruitment and overdistension and tidal hyperinflation in an animal model of ARDS. Open lung PEEP, defined as the one corresponding to the maximal value of Xrs, maximized oxygenation minimizing the amount of derecruited lung tissue. Open lung PEEP also minimized intratidal overdistension, defined as a within-breath reduction of Xrs. Finally we evaluated whether a PEEP titration strategy based on optimal Xrs is able to reduce the incidence of VILI with respect to a standard oxygenation-based protocol. In an animal model of ARDS we found that a Xrs-based ventilatory strategy resulted in higher levels of PEEP, improved compliance and oxygenation, and reduced systemic and pulmonary arterial pressure compared to a standard oxygenation-based protocol. Moreover, after 12 hours of ventilation a lower concentration of inflammatory markers and lower histological signs of lung

injury were observed in the group of animals ventilated according to Xrs. High Frequency Oscillatory Ventilation (HFOV) provides an attractive alternative to conventional mechanical ventilation being by definition lung protective. However HFOV has a beneficial effect over conventional ventilation only when a proper continuous distending pressure (CDP) is used. We investigated the possibility to apply FOT during HFOV. At first we evaluated the accuracy of Zrs obtained from the analysis the pressure and flow signals measured at the airways opening during HFOV. Although the accurate assessment of Zrs requires small amplitude pressure stimuli, we found a very strong linear correlation between Xrs measured during HFOV and during traditional FOT. This result suggests that the CDP value that maximises Xrs can be identified during HFOV without altering the ventilatory pattern and without requiring any additional device. By comparing the optimal CDP according to Xrs and to the optimal CDP according to the static P-V curve we found a good agreement between the two methods. Ventilation modalities with high distending pressures may induce pulmonary edema, which is preceded by interstitial edema. Since the transition from interstitial to severe edema is a rapid phenomenon characterized alveolar flooding, it would be important to monitor fluid accumulation in lung parenchyma. We found that Xrs is very sensible to the development of interstitial edema. Moreover using a

composite low frequency FOT stimulus, combined with a mathematical model, we were able to separate the airways and tissue contribution to total Zrs and to differentiate between different phenomena such as derecruitment of alveolar units or regional heterogeneities in lung function. We concluded that the continuous monitoring of Zrs in subjects at risk of developing pulmonary edema is able to early identify the accumulation of interstitial lung fluid.

The results of the experimental studies performed on animal models of lung injury encouraged us in applying FOT for the management of ventilated patients. Thus we performed a clinical study on preterm newborns receiving conventional mechanical ventilation. We found that Xrs measured at 5 Hz is very sensitive to changes in PEEP and posture. Premature infants receiving ventilation present very heterogeneous characteristics depending on the degree of immaturity and the duration of ventilatory support. The PEEP dependency of Xrs was found to provide significant information about the pathological features of the lung disease. This information is crucial for the physician for the choice of the proper ventilatory strategy for each individual patient. Xrs was also significantly dependent on the infant's posture. Xrs was found to be higher in prone position than in supine position and in head tilt up compared to the horizontal position. Continuous positive airways pressure (CPAP) is the most common form of ventilatory

support in infant RDS. However in infants CPAP is delivered through nasal prongs, so it is impossible to connect to the airways opening without leaks. Moreover, different levels of CPAP have found to affect end-expiratory lung volume and thoraco-abdominal asynchrony that cannot be assessed by FOT. Optoelectronic plethysmography allows the assessment of chest wall volume changes through the measurement of the thoraco-abdominal surface motion, without requiring a connection to the airways opening. This technique has been widely used in adults. In the present study we developed measurement protocols and geometrical models for its application to newborns.

In conclusion FOT is a very promising tool for the continuous monitoring and the management of ventilated patients. In fact it can be used for the titration of ventilatory parameters in different ventilatory modalities, to evaluate the effect of different interventions such as recruitment manoeuvres or changes in position, and to monitor the development of ventilation associated complications such as interstitial lung edema. OEP may be useful for the assessment of changes in lung volumes, including end-expiratory lung volume, of breathing pattern and of thoraco-abdominal asynchronies, in clinical situations in which airways opening flow cannot be measured, like in infants supported by CPAP.